

# Optimization and Stabilization of Functional Renormalization Group Flows

Niklas Zorbach  <sup>1,\*</sup> Jonas Stoll  <sup>1,†</sup> and Jens Braun  <sup>1,2,‡</sup>

<sup>1</sup> Technische Universität Darmstadt, Department of Physics, Institut für Kernphysik, Theoriezentrum, Schlossgartenstraße 2, D-64289 Darmstadt, Germany

<sup>2</sup> ExtreMe Matter Institute EMMI, GSI, Planckstraße 1, D-64291 Darmstadt, Germany

We revisit optimization of functional renormalization group flows by analyzing regularized loop integrals. This leads us to a principle, the *Principle of Strongest Singularity*, and a corresponding order relation which allows to order existing regularization schemes with respect to the stability of renormalization group flows. Moreover, the order relation can be used to construct new regulators in a systematic fashion. For studies of critical behavior, which require to follow renormalization group flows down to the deep infrared regime, such new regulators may turn out to be particularly useful. The general application of this principle is demonstrated with the aid of a scalar field theory which is solved over a wide range of scales with novel methods borrowed from numerical fluid dynamics.

## I. INTRODUCTION

In quantum field theory, the computation of observables in general requires to introduce a regularization. Of course, any physical observable  $\mathcal{O}$  should be independent of the chosen regularization scheme  $R$ , i.e.,

$$\frac{\delta \mathcal{O}}{\delta R} = 0. \quad (1)$$

Strictly speaking, however, this independence of the regularization scheme only holds for the exact result for  $\mathcal{O}$ . In practice, the computation of observables requires a truncation of the quantum effective action  $\Gamma$  of some kind. In a truncated calculation, it then appears natural to search for an optimal regularization scheme which brings the results as close as possible to the *a priori* unknown exact results for the observables under consideration.

The optimization of the computation of the effective action and derived observables with respect to the regularization scheme has been discussed intensely over decades now and its origin may be dated back to the seminal work by Stevenson on optimized perturbation theory and the introduction of the Principle of Minimum Sensitivity (PMS) [1]. Loosely speaking, this principle relies on the assumption that the optimal scheme defines a stationary point of an observable or a given set of observables under the variation of the regularization scheme.

In the context of the functional Renormalization Group (RG) framework, which also underlies our present analysis, the starting point for the computation of any observable is the Wetterich equation [2]:

$$\partial_t \Gamma_k[\Phi] = \frac{1}{2} \text{STr} \left[ \left( \Gamma_k^{(2)}[\Phi] + R_k \right)^{-1} \cdot \partial_t R_k \right]. \quad (2)$$

Here,  $\Gamma_k[\Phi]$  denotes the scale-dependent (i.e., coarse-grained) effective average action. The supertrace arises

since the field  $\Phi$  of a given theory may in general contain both bosonic and fermionic degrees of freedom and therefore provides a minus sign in the fermionic subspace. The regulator function  $R_k$  depends on the infrared (IR) cutoff scale  $k$  and defines the regularization scheme. The RG time is related to the scale  $k$  via  $t = -\ln(k/\Lambda)$  with  $\Lambda$  being the ultraviolet (UV) scale.

Optimization of RG flows has already been discussed early on by means of a PMS-like criterion in Ref. [3]. In the context of the functional RG approach, PMS and the associated optimization have been considered and employed in computations of critical exponents of scalar field theories, see, e.g., Refs. [4, 5]. For a more recent discussion, including computations of universal amplitude ratios, we refer to Refs. [6–9]. A first detailed and general discussion of optimization of functional RG flows has been given by Litim in a series of ground-breaking articles [10–12]. Litim’s optimization criterion is based on a maximization of the gap in the regularized two-point function in the RG flow and encompasses PMS as a special case. In fact, the optimization introduced by Litim is more general and the underlying criterion eventually leads to an improved convergence of the RG flow, see also Ref. [13]. Studies of critical exponents based on Litim’s optimization criterion can be found in Refs. [14–17].

In a seminal analysis of optimization of functional RG flows [13], Pawłowski then showed that, loosely speaking, Litim’s criterion for the construction of an optimized regulator based on the maximization of the gap in the propagator has to be supplemented by the minimization of the full (regularized) two-point function entering the flow equation (2) to obtain optimized regulators for truncations at any given order  $n$  of the derivative expansion.<sup>1</sup>

Phenomenologically speaking, the optimization discussed by Litim and Pawłowski aims at a minimization of the deviation of the values of observables computed with a given truncation from their exact values. For example, this approach to optimization of RG flows can

\* [niklas.zorbach@tu-darmstadt.de](mailto:niklas.zorbach@tu-darmstadt.de)

† [jonas.stoll@tu-darmstadt.de](mailto:jonas.stoll@tu-darmstadt.de)

‡ [jens.braun@tu-darmstadt.de](mailto:jens.braun@tu-darmstadt.de)

<sup>1</sup> This minimization requires to compute the norm of the full propagator on Sobolev spaces  $H_n$  with  $n \in \mathbb{N}$ .

be employed to improve computations of critical exponents but also underlies other type of studies, such as an early study of the deconfinement phase transition in Yang-Mills theory [18]. Note that a prescription for the construction of such optimized regulators based on a suitable definition of the length of RG trajectories can be found in Ref. [19]. Last but not least, we add that it has more recently also been proposed to optimize functional RG flows by employing constraints originating from conformal invariance [20, 21].

The optimization criterion discussed in our present work aims at an improvement of the stability of functional RG flows in the presence of spontaneous symmetry breaking and emerges from an analysis of RG flows computed with techniques borrowed from the field of numerical fluid dynamics, which provide an intuitive picture of the dynamics of RG flows in terms of advection-diffusion equations [22–27].

In case of theories featuring spontaneous symmetry breaking, convexity of the effective action implies the emergence of a flat region in field space in the RG flow which may eventually cause numerical precision problems, i.e., breakdowns of RG flows at (comparatively large) finite RG scales. In general, the precise value of this breakdown scale depends on the chosen regulator. In the present work, we show that the stability of the RG flow in such a situation is directly related to the strength of the singularities of the *regularized* loop integrals in the regime of negative mass parameters. This naturally results in the definition of an order relation on the space of regulators. To illustrate this, we employ the so-called local potential approximation (LPA), the zeroth-order of the derivative expansion of the effective action. However, our line of arguments is not bound to this approximation but is more general, as we shall discuss right at the very beginning in Sec. II. There, we introduce the principle underlying our optimization, the Principle of Strongest Singularity (POSS), as well as the associated order relation. In Sec. III, we employ this principle to discuss regulator functions and also to construct new regulators as concrete examples for the application of this principle. In Sec. IV, we then numerically test the stability of RG flows obtained from these new regulators and also from other existing regulators by computing the RG flow of the effective potential of a simple scalar field theory in LPA. Our conclusions can be found in Sec. V.

## II. PRINCIPLE OF STRONGEST SINGULARITY

### A. General Analysis

In the derivation of the Wetterich equation (2) one tacitly assumes that the scale-dependent full propagator,

$$G_k[\Phi] = \left( \Gamma_k^{(2)}[\Phi] + R_k \right)^{-1}, \quad (3)$$

exists for all  $k > 0$ . From an analysis of the general form of the Wetterich equation, it follows that this assumption is justified. Indeed, the RG flow generated by the Wetterich equation is such that it tends to push the inverse propagator away from potentially existing points with eigenvalue zero. This becomes more apparent by realizing that the Wetterich equation (2) is of the form

$$\partial_t \Gamma_k \propto - \det \left( \Gamma_k^{(2)}[\Phi] + R_k \right)^{-1}. \quad (4)$$

Note that we have defined the RG time to be a positive quantity,  $t = -\ln(k/\Lambda) > 0$ , and that  $\det G_k > 0$  since the eigenvalues of the operator in Eq. (3) are positive. Thus, if the RG flow approaches a point associated with zero eigenvalues, then the determinant of the inverse scale-dependent propagator becomes smaller and smaller. This may be considered as a “self-healing” property of the Wetterich equation since it eventually prevents the RG flow from reaching a point with zero eigenvalues. Note that the appearance of zero eigenvalues in the eigenvalue spectrum of the inverse propagator is intimately connected with the formation of a convex effective action, see also Ref. [28]. In particular, we encounter this scenario in theories which develop a nontrivial minimum of the effective action in the RG flow that survives in the IR limit, i.e., theories featuring spontaneous symmetry breaking. The focus of the present work is exactly on this class of theories. In any case, since the inverse scale-dependent propagator depends on the regulator, it is clear that the regulator choice affects the “strength” of the singular behavior close to the zero eigenvalues of the inverse propagator. Below, this observation leads us to the Principle of Strongest Singularity. The underlying idea is that regulators, which generate RG flows with *optimized* self-healing properties, eventually yield more stable RG flows. Based on this principle, we shall also introduce an order relation which allows to compare regulators in a meaningful manner.

Before we can quantitatively compare different regulator schemes, we have to introduce a *comparability condition*. To this end, we consider a theory with spontaneous symmetry breaking and assume that  $\Gamma_k$  is a *generic* reference solution of the Wetterich equation (2) obtained with a given reference regulator  $R_k$ . Then, there exists at least one field configuration  $\Phi_0$  where the determinant of the inverse scale-dependent propagator vanishes in the IR limit,  $k \rightarrow 0$ :<sup>23</sup>

$$\lim_{k \rightarrow 0} \det \left( \frac{1}{k^2} (\Gamma_k^{(2)}[\Phi_0] + R_k) \right) = 0, \quad (5)$$

<sup>2</sup> Since the effective action becomes convex in the IR limit [28], there in general exists a set of values of  $\Phi$  for which the determinant in Eq. (5) vanishes.

<sup>3</sup> The factor  $1/k^2$  in Eq. (5) is necessary to render the determinant dimensionless at least for bosonic fields.

i.e., the full inverse propagator can not be inverted at  $\Phi_0$  in this limit. Now let  $\tilde{R}_k$  be a regulator which differs from  $R_k$ . We then say that the regulator  $\tilde{R}_k$  is *comparable* to  $R_k$ , if

$$\lim_{k \rightarrow 0} \det \left( \frac{1}{k^2} (\Gamma_k^{(2)}[\Phi_0] + \tilde{R}_k) \right) = 0 \quad (6)$$

for the same field configuration  $\Phi_0$ , i.e., we do *not* have

$$\lim_{k \rightarrow 0} \det \left( \frac{1}{k^2} (\Gamma_k^{(2)}[\Phi_0] + \tilde{R}_k) \right) > 0 \quad (7)$$

or

$$\lim_{k \rightarrow k_c > 0} \det \left( \frac{1}{k^2} (\Gamma_k^{(2)}[\Phi_0] + \tilde{R}_k) \right) = 0 \quad (8)$$

for a nonzero  $k_c$ . We emphasize that  $\Gamma_k$  is a solution of the Wetterich equation with respect to  $R_k$  not  $\tilde{R}_k$ . In Eq. (6), we simply state that a combination of a given  $\Gamma_k$  obtained from a given regulator with another regulator  $\tilde{R}_k$  does not alter the limiting behavior (5).

With this comparability condition at hand, we can now compare how different regulators behave with respect to a given reference solution  $\Gamma_k$  in the IR limit. A first guess for an order relation for regulators on the space of all comparable regulators would be to compare how “fast” the determinant at a given field configuration  $\Phi_0$  vanishes. Loosely speaking, a regulator yielding a rapidly vanishing determinant is associated with a stronger singular behavior close to  $\Phi_0$  on the right-hand side of the Wetterich equation, see Eq. (4). Consequently, such a stronger singular behavior improves the self-healing property of the RG flow and hence its stability. However, this reasoning ignores the exact form of the Wetterich equation. A meaningful comparison is obtained by considering the full right-hand side of the Wetterich equation in the IR limit. Assume  $R^A$  and  $R^B$  are comparable to a given  $R_k$  according to our definition above, then we can define an order relation as follows:

$$\mathcal{R}(R^A, R^B) = \lim_{k \rightarrow 0} \frac{\text{STr} \left( (\Gamma_k^{(2)}[\Phi_0] + R_k^A)^{-1} \cdot \partial_t R_k^A \right)}{\text{STr} \left( (\Gamma_k^{(2)}[\Phi_0] + R_k^B)^{-1} \cdot \partial_t R_k^B \right)}. \quad (9)$$

Recall again that  $\Gamma_k$  is a reference solution of the Wetterich equation obtained with a given reference regulator  $R_k$ . If  $\mathcal{R}(R^A, R^B) > 1$  the singularity of  $R^A$  is stronger than of  $R^B$  and, in turn, yields a more stable RG flow. We shall therefore write  $R^A > R^B$  (i.e.,  $R^A$  is *more stable than*  $R^B$ ) if  $\mathcal{R}(R^A, R^B) > 1$  and  $R^A < R^B$  (i.e.,  $R^A$  is *less stable than*  $R^B$ ) if  $\mathcal{R}(R^A, R^B) < 1$ . Hence,  $\mathcal{R}$  defines an order relation which is reflexive, transitive and strongly connected.<sup>4</sup>

## B. Local potential approximation

In this subsection, we would like to *illustrate* the application of the Principle of Strongest Singularity and the associated order relation (9) with the aid of a concrete example. To be specific, we shall consider a scalar field theory in  $d$  spacetime dimensions in LPA. The classical action is given by

$$S[\phi] = \int d^d x \left\{ \frac{1}{2} (\partial_\mu \phi)^2 + \frac{1}{2} m^2 \phi^2 + \frac{1}{4} \lambda \phi^4 \right\}, \quad (10)$$

where  $\phi$  is a real-valued scalar field. This action serves as the initial condition for our ansatz for the scale-dependent effective action  $\Gamma_k$ :

$$\Gamma_k[\phi] = \int d^d x \left\{ \frac{1}{2} (\partial_\mu \phi)^2 + U_k(\phi) \right\}. \quad (11)$$

For  $k \rightarrow \Lambda$ , we have  $\Gamma_k \rightarrow S$ . By plugging this ansatz into the Wetterich equation, see Eq. (2) and evaluating it then on a constant field configuration  $\phi$ , we obtain the flow equation for the scale-dependent effective potential  $U_k$ . For concreteness, we shall restrict ourselves to regulators of the form  $R_k(p, q) \propto R_k(p^2) \delta^{(d)}(p+q)$ , where  $R_k(p^2) = p^2 r(p^2/k^2)$  can be expressed through a dimensionless regulator shape function  $r(y)$  with  $y = p^2/k^2$  and  $p^2 = p_0^2 + p_1^2 + \dots + p_{d-1}^2$ .

An illustrative analysis of the stability of RG flows for this model based on POSS can be found in Sec. IV. In the following, however, we shall first focus on a general discussion of POSS in LPA and derive the order relation for regulators in this approximation. For this discussion, it is convenient to introduce the following auxiliary quantity:

$$P^2(y) = y(1 + r(y)). \quad (12)$$

From this object, we can construct the so-called threshold functions which correspond to one-particle irreducible one-loop diagrams and appear as the fundamental building blocks in the flow equations of, e.g., the effective potential and the couplings. The regularization-scheme dependence of the flow equations is solely encoded in these functions. In a calculation of the effective potential in LPA, they are of the form

$$I_m^{(d)}(\omega) = \int_0^\infty dy I_m^{(d)}(\omega, r(y), r'(y), y) \quad (13)$$

with

$$I_m^{(d)}(\omega, r(y), r'(y), y) = -y^{\frac{d}{2}+1} \frac{\partial_y r(y)}{(P^2(y) + \omega)^m} \quad (14)$$

and  $m \geq 1/2$ . As such they are functionals of  $r(y)$  or equivalently, of  $P^2(y)$  because of Eq. (12). The parameter  $m$  “measures” the number of internal lines of the threshold function. The parameter  $\omega$  plays the role of an effective (potentially field-dependent) dimensionless mass term. For example, in our scalar field theory, the

<sup>4</sup> In general, this order relation depends on  $\Phi_0$  and on the reference RG flow  $\Gamma_k$  associated with a corresponding reference regulator  $R_k$ . By using a different reference flow or a different field configuration  $\Phi_0$ , we could in principle obtain a different order relation.

parameter  $\omega$  is essentially given by the second derivative of the effective potential with respect to the field, i.e.,  $\omega = \partial_\phi^2 U_k(\phi)/k^2$ .

With the threshold functions at hand, the flow equation for the scale dependent effective potential  $U_k$  assumes the following form:<sup>5</sup>

$$\partial_t U_k(\phi) = -\frac{1}{2} \frac{\text{surf}(d)k^d}{(2\pi)^d} l_1^{(d)}(\omega), \quad (15)$$

where  $\text{surf}(d)$  is the surface of a  $d$ -dimensional ball with radius one. To be specific, we have  $\text{surf}(d)/d = \text{vol}(d) = 2\pi^{d/2}/(d\Gamma(d/2))$ .

We can now apply the comparability condition (6) from Sec. II to LPA. To this end, we first have to determine the full inverse regularized propagator evaluated for some reference field configuration. We choose  $\Phi_0 = \phi = 0$ , being a simple choice for studies of models featuring a nontrivial minimum of the effective action in the IR limit:

$$\begin{aligned} & \Gamma_{k,pq}^{(2)}[0] + R_{k,pq} \quad (16) \\ &= (p^2 + \partial_\phi^2 U_k(0) + p^2 r(p^2/k^2))(2\pi)^d \delta^{(d)}(p+q). \end{aligned}$$

Using the definition (12), the (dimensionless) determinant reads

$$\begin{aligned} & \det\left(\frac{1}{k^2}(\Gamma_{k,pq}^{(2)}[0] + R_{k,pq})\right) \\ &= \prod_{p_0, \dots, p_{d-1}} (P^2(y) + \partial_\phi^2 U_k(0)/k^2). \end{aligned}$$

Assuming that the potential develops a nontrivial minimum  $\phi_{\min}$  in the RG flow, convexity of the effective action in the IR limit requires the determinant to vanish at  $\phi = 0$  for  $k \rightarrow 0$ , implying that  $\omega_0(k) = \partial_\phi^2 U_k(0)/k^2$  approaches  $\omega_{\text{pole}}$ ,

$$\omega_{\text{pole}} = -\min_{0 \leq y \leq \infty} P^2(y), \quad (17)$$

in this limit.

From Eq. (6), it now follows that a different regulator  $\tilde{R}$  parametrized by the shape function  $\tilde{r}$  is comparable to the regulator  $R$  parametrized by the shape function  $r$ , if  $\tilde{P}^2(y)$  associated with  $\tilde{r}$  yields the same  $\omega_{\text{pole}}$  in Eq. (17). In addition, from a comparison of Eq. (4) with Eq. (15), we deduce that the threshold functions (13) should diverge in the limit  $\omega_0 \rightarrow \omega_{\text{pole}}$  but remain finite for  $\omega_0 > \omega_{\text{pole}}$ . This singularity of the threshold functions essentially governs the “self-healing” property of the RG flow mentioned in Sec. II and controls the approach of the effective potential to a convex function in the IR limit.

<sup>5</sup> In terms of concrete models, for example, this flow equation describes the scalar contribution to the RG flow of the effective potential in the Gross-Neveu-Yukawa model, see, e.g., Ref. [29], but it may also be employed to study critical behavior in the Ising model.

As already indicated above, the existence of this singularity is necessary for the effective potential to become convex in studies where the ground state is governed by spontaneous symmetry breaking, see also Refs. [28, 30].

To summarize, we deduced from the comparability condition (6) that  $\omega_{\text{pole}}$  must assume the same value for any two regulators in order to render them comparable, and as a consequence, the position of the singularity of the threshold functions must also be the same. In the following we choose  $\omega_{\text{pole}} = -1$  without loss of generality and consider only regulators  $R$  which fulfill

$$\min_{0 \leq y \leq \infty} P^2(y) = 1. \quad (18)$$

Note that this relation defines a *normalization condition* in the sense that *any* regulator  $R$  of the form  $R_k(p^2) = p^2 r(p^2/k^2)$  can be *normalized* such that it satisfies Eq. (18) and hence can be rendered comparable. In fact, this can be achieved by exploiting the freedom that we can rescale the unphysical RG scale  $k$ . To be explicit, let us consider a one-parameter family of regulators parameterized by  $\xi \in \mathbb{R}_{>0}$ ,  $r_\xi(y) := r(\xi y)$ . From the dependence of the flow equation on the regulator, it then follows that the scale-dependent effective actions obtained from calculations with  $r_{\xi=1}$  and  $r_\xi$  are directly related:<sup>6</sup>

$$\Gamma_k \equiv \Gamma_k^{(\xi=1)} = \Gamma_{\sqrt{\xi}k}^{(\xi)},$$

provided that the initial conditions are chosen accordingly, i.e.,

$$S \equiv \Gamma_\Lambda = \Gamma_{\sqrt{\xi}\Lambda}^{(\xi)}.$$

Loosely speaking, a change of  $\xi$  can be compensated by “compressing” or “stretching” the RG flow between a given starting point and endpoint. From this, it follows that the results in the IR limit  $k \rightarrow 0$  do not depend on  $\xi$ . In this sense, regulators of the one-parameter regulator family are *equivalent*. On the other hand,

$$P_\xi^2(y) = \frac{1}{\xi} P_{\xi=1}^2(\xi y), \quad (19)$$

where  $P_\xi^2(y) = y(1 + r_\xi(y))$ . If  $y_0$  is now a global minimum of  $P_\xi^2(y)$ , then  $P_{\xi=1}^2(y)$  has a global minimum at  $y = \xi y_0$  and we find  $\min_y P_{\xi=1}^2(y) = \xi \min_y P_\xi^2(y)$ . Thus, any regulator  $R$  of the types considered in this work can be normalized by choosing an appropriate  $\xi$  and hence can be made comparable with respect to Eq. (6).

With these considerations at hand, we obtain the following order relation from Eq. (9) in LPA:

$$\mathcal{R}(r_A, r_B) = \lim_{k \rightarrow 0} \frac{l_1^{(d)}(\omega_0(k), r_A)}{l_1^{(d)}(\omega_0(k), r_B)} \quad (20)$$

<sup>6</sup> This is also correct in cases where only a truncation of the full effective action is considered, such as LPA in this subsection.

$$= \lim_{\omega \rightarrow -1} \frac{l_1^{(d)}(\omega, r_A)}{l_1^{(d)}(\omega, r_B)}$$

with  $\omega_0(k) = \partial_\phi^2 U_k(0)/k^2$ . Here, we have removed the explicit dependence on  $k$  in the last step, which is possible since the limit  $k \rightarrow 0$  is equivalent to the limit  $\omega \rightarrow -1$  according to our choice for  $\omega_{\text{pole}}$  above. In the special case of LPA, the details of the RG flow, i.e., how  $\omega_0(k) = \partial_\phi^2 U_k(0)/k^2$  eventually approaches  $\omega_{\text{pole}}$ , are irrelevant. Thus, no explicit reference RG flow and no reference regulator is required for the order relation, in contrast to the general formulation in Eq. (9). This implies that, in LPA, POSS effectively only compares the behavior of the threshold functions (for different regulators) close to the singularity with each other.

In Sec. IV, we shall indeed demonstrate that a more stable regulator, i.e., a regulator with a stronger self-healing property, generates a more stable RG flow which means that the scale-dependent effective potential becomes flat faster in terms of RG time in the IR limit. More precisely, for  $r_A > r_B$ , we have  $\omega_0(r_A, k) > \omega_0(r_B, k)$  for  $k \rightarrow 0$ , provided that the RG flows associated with the two regulators approach the same IR limit. Furthermore, we show that an RG flow generated by a stable regulator can be solved down to much smaller RG scales without numerical breakdowns than it is the case for less stable regulators. In this spirit, more stable regulators generate *numerically* more stable RG flows.

Note that the order relation (20) depends on the number  $d$  of spacetime dimensions. We shall discuss this dependence in more detail in Subsec. III B. The independence of the parameter  $m$  follows from L'Hôpital's rule.

Finally, we would like to add that, for a more general theory including (multiple) bosonic and fermionic degrees of freedom, the order relation effectively boils down to the one which dominates the order relation (9) in the IR limit. This is a consequence of the fact that the flow equation for the effective action is simply a sum of the loops associated with the various degrees of freedom.

### III. CONSTRUCTION OF REGULATORS

Following POSS and the corresponding order relation, we shall now construct regulators which yield (numerically) stable RG flows for studies of simple scalar field theories in LPA.

In the first subsection, we start by discussing general constraints for the regulator shape function  $r$ . These constraints can be deduced from the derivation of the Wetterich equation and the properties of the threshold functions discussed in Subsec. II B. In the second subsection, we aim at providing an intuitive understanding of what actually determines the “strength” of the singularity of the threshold function at  $\omega_{\text{pole}} = -1$ . This is useful since the properties of this singularity control the (numerical) stability of the RG flows as we shall demonstrate explicitly in Sec. IV. Based on these considerations,

we finally construct new regulators in the third subsection and compare them to frequently used ones.

#### A. Constraints for regulator functions

Let us begin with a discussion of general properties of regulators. The (regulator) function  $R_k(p^2)$  entering the Wetterich equation has to obey the following three conditions [2]:

$$\lim_{k \rightarrow 0} R_k(p^2) = 0, \quad (21)$$

$$\lim_{k \rightarrow \infty} R_k(p^2) = \infty, \quad (22)$$

and

$$\lim_{p \rightarrow 0} R_k(p^2) > 0 \quad (23)$$

for  $k > 0$ . The first condition guarantees that the regulator is removed in the IR limit,  $k \rightarrow 0$ , such that we recover the quantum effective action  $\Gamma$ . The second condition ensures that the coarse-grained effective action  $\Gamma_k$  approaches the classical action  $S$  in the limit  $k \rightarrow \infty$ . Finally, the third condition ensures that IR divergences in the loop integrals are removed, loosely speaking, by inserting a scale-dependent and momentum-dependent mass term into the propagator. In terms of the regulator shape function  $r$  and the dimensionless variable  $y = p^2/k^2$  the three conditions are fulfilled by only two conditions, namely

$$\lim_{y \rightarrow 0} y r(y) > 0, \quad \lim_{y \rightarrow \infty} r(y) = 0. \quad (24)$$

Equivalently, in terms of the auxiliary quantity  $P^2$  introduced in Eq. (12), we have

$$\lim_{y \rightarrow 0} P^2(y) > 0, \quad \lim_{y \rightarrow \infty} \frac{P^2(y)}{y} = 1. \quad (25)$$

We would like to emphasize that the conditions given in Eq. (24), or equivalently in Eq. (25), are in general not sufficient to guarantee finiteness of the threshold functions  $l_m^{(d)}$  for  $\omega > \omega_{\text{pole}}$ . Also, these conditions are not sufficient to guarantee that these functions diverge at  $\omega = \omega_{\text{pole}}$ , see also Sec. III B. Therefore, it is necessary to introduce additional constraints for the regulator  $r$  which depend on, e.g., the number  $d$  of spacetime dimensions, the parameter  $m$ , and on the position of the poles of  $I_m^{(d)}$ . For a more detailed discussion we refer the reader to Appendix A, where we also show that the often used exponential regulator  $r_{\text{exp}}$  does not yield threshold functions which diverge at  $\omega_{\text{pole}}$  in  $d > 2$  spacetime dimensions, at least for  $m = 1$ , and hence this regulator spoils the “self-healing” property of the RG flow discussed in Sec. II, in accordance with Ref. [30]. From here on, we shall restrict our discussion to regulators  $r$  which yield threshold functions compatible with all the aforementioned constraints.

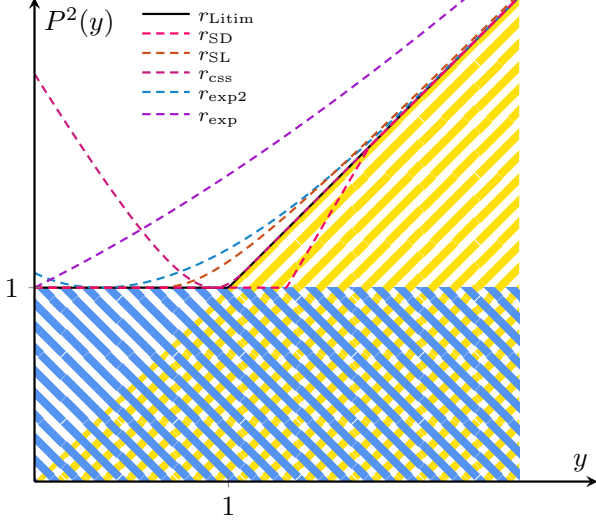


FIG. 1. Illustration of  $P^2(y)$  (corresponding to the regularized squared  $d$ -momentum in  $d$  spacetime dimensions), see Eq. (12), for a selected set of normalized regulators listed in Tab. I. The black line corresponds to the Litim regulator, see Eq. (28). The blue shaded region is forbidden by the normalization condition (18). In the yellow shaded region the regulator shape function becomes negative,  $r(y) < 0$ .

In general, regulators where the threshold function  $l_m^{(d)}$  becomes negative for some value of  $\omega$  generate instabilities in the RG flow. This can be better understood by looking at the flow equation (15) from a fluid-dynamical standpoint [22–27]. It then becomes clear that a negative threshold function entails a *violation* of the diffusion property of the flow equation, see Eq. (51) and also the corresponding discussion below. Hence, appropriate regulators should be elements of the set  $\mathcal{A}'$ , where

$$\mathcal{A}' = \{r \mid r \text{ normalized and continuous piecewise differentiable with } l_m^{(d)}(\omega) \geq 0 \text{ for all } \omega \in (-1, \infty)\}. \quad (26)$$

The integrands of the threshold functions can only become negative if  $r'(y) > 0$  for some value of  $y$ . Therefore, for simplicity, one may only consider regulators from the set  $\mathcal{A}$  with

$$\mathcal{A} = \{r \mid r \text{ normalized and continuous piecewise differentiable with } r' \leq 0\} \subset \mathcal{A}'. \quad (27)$$

This is the set of regulator functions usually considered in the context of functional RG studies. We add that the restriction to  $\mathcal{A}$  also prevents  $P^2$  from entering the yellow shaded region in Fig. 1, i.e., it prevents  $r$  from becoming negative. Thus, with respect to our normalization condition (18), all regulators in  $\mathcal{A}$  are “living” inside the unshaded region in Fig. 1 and have at least one point

### Regulator

$r_{\exp}(y) = \frac{1}{\exp(y)-1}$	Ref. [2]
$r_{\text{mexp}}(y) = \frac{3.92}{e^{\ln(1+3.92)y-1}}$	Ref. [10]
$r_{\exp2}(y) = \frac{1}{1-e^{-y-y^2}} - 1$	–
$r_{\text{css}}(y) = \frac{c_1}{\exp(c_2 y^b/(1-y^b))-1} \theta(1-y)$	Ref. [31]
$r_{\text{Litim}}(y) = \left(\frac{1}{y} - 1\right) \theta(1-y)$	Ref. [11]
$r_{\text{NSL}}(y) = \left(\frac{1}{y} - 1\right) \left(\frac{1}{2} \tanh(\epsilon(1-y)) + \frac{1}{2}\right)$	Eq. (43)
$r_{\text{SL}}(y) = \exp\left(-\frac{1}{y-\frac{1}{2}}\right) \theta\left(y - \frac{1}{2}\right) + \frac{1}{y} - 1$	Eq. (44)
$r_{\text{SD}}(y) = \begin{cases} \frac{1}{y} - 1 & \text{for } 0 \leq y < y_0 \\ \frac{s(y-y_0)+1}{y} - 1 & \text{for } y_0 \leq y < \frac{1-sy_0}{1-s} \\ 0 & \text{for } \frac{1-sy_0}{1-s} \leq y \end{cases}$	Eq. (46)
$r_{x_0}(y) = \frac{((1-x_0)e^{x_0-y}+y-1)\theta(y-x_0)+1}{y} - 1$	Eq. (47)
$r_{\text{osc}}(y) = \theta(1-y)(A(1 - \cos(2\pi ny)) - y + 1) + y$	Eq. (48)

TABLE I. List of various regulator shape functions. All regulators are in  $\mathcal{A}$ , except for  $r_{\text{SD}}$  and  $r_{\text{NSL}}$  which are in  $\mathcal{A}' \setminus \mathcal{A}$ . Note that the regulator shape functions  $r_{\text{mexp}}$ ,  $r_{\exp2}$ ,  $r_{\text{css}}$ , and  $r_{\text{NSL}}$  as listed here are not normalized according to Eq. (18).

of contact with the line defined by  $P^2(y) = 1$ . The black line in Fig. 1 represents the so-called Litim regulator [11],

$$r_{\text{Litim}}(y) = \left(\frac{1}{y} - 1\right) \theta(1-y). \quad (28)$$

For this regulator,  $P^2$  as a function of  $y$  agrees identically with the boundary of the unshaded region in Fig. 1. Below, we shall show that this regulator is the one which exhibits the strongest singular behavior for regulators in  $\mathcal{A}$ .

In the following we shall discuss various examples of regulators which are summarized and categorized in terms of the sets  $\mathcal{A}$  and  $\mathcal{A}'$  in Tab. I.

### B. Principle of Strongest Singularity and a simple area law

By looking at the definition of the threshold functions in Eq. (14), we observe that a larger area under the curve defined by the function  $I_m^{(d)}$  directly corresponds to a stronger singular behavior of the threshold functions close to  $\omega_{\text{pole}} = -1$ , see Eq. (20). In the following we shall discuss the dependence of the size of this area on  $P^2(y)$ , i.e.,  $r(y)$ . In particular, we shall show that the minima of  $P^2(y)$  play a crucial role since they essentially determine the size of the area in the limit  $\omega \rightarrow -1$ .

and therefore the strength of the singular behavior of the associated threshold function.

Let us begin by considering a normalized regulator which is at least continuously differentiable *once* and has a unique global minimum of  $P^2(y)$  at  $y_0 \in (0, 1)$ . At  $y_0$ , the value of the regulator as well as its derivative agree with the corresponding ones of the Litim regulator by construction:

$$r(y_0) = r_{\text{Litim}}(y_0) \quad \text{and} \quad r'(y_0) = r'_{\text{Litim}}(y_0). \quad (29)$$

Thus, the integrand of the generic threshold function defined in Eq. (14) agrees with the one obtained from the Litim regulator at  $y_0$  (for any number of spacetime dimensions), i.e., we have

$$\begin{aligned} I_m^{(d)}(\omega, r(y_0), r'(y_0), y_0) \\ = I_m^{(d)}(\omega, r_{\text{Litim}}(y_0), r'_{\text{Litim}}(y_0), y_0). \end{aligned} \quad (30)$$

Close to  $y_0$ , i.e., for sufficiently small  $\epsilon > 0$ , we find

$$r(y_0 \pm \epsilon) > r_{\text{Litim}}(y_0 \pm \epsilon), \quad (31)$$

$$r'(y_0 + \epsilon) > r'_{\text{Litim}}(y_0 + \epsilon), \quad (32)$$

$$r'(y_0 - \epsilon) < r'_{\text{Litim}}(y_0 - \epsilon). \quad (33)$$

This immediately implies that

$$\begin{aligned} I_m^{(d)}(\omega, r(y_0 + \epsilon), r'(y_0 + \epsilon), y_0 + \epsilon) \\ < I_m^{(d)}(\omega, r_{\text{Litim}}(y_0 + \epsilon), r'_{\text{Litim}}(y_0 + \epsilon), y_0 + \epsilon). \end{aligned} \quad (34)$$

Since we assumed that  $r(y)$  has only one point of contact with the Litim regulator shape function at  $y_0 \in (0, 1)$ , we can conclude that

$$I_m^{(d)}(\omega, r(y), r'(y), y) < I_m^{(d)}(\omega, r_{\text{Litim}}(y), r'_{\text{Litim}}(y), y) \quad (35)$$

for all  $y \in (y_0, 1]$ . For values  $y \in [0, y_0)$ , we can in general not find a corresponding inequality. There, the denominator and the numerator of the integrand (14) nontrivially compete with each other, such that the integrand can exceed the values obtained with the Litim regulator. However, in the limit  $\omega \rightarrow -1$ , the latter is not the case anymore. To show this, it is convenient to introduce the following auxiliary function:

$$\bar{I}_m^{(d)} := (1 + \omega)^m I_m^{(d)}. \quad (36)$$

This function is no longer singular and therefore the integration with respect to  $y$  yields a function which is well-defined in the limit  $\omega \rightarrow -1$ . For any  $y$  with  $P^2(y) > 1$ ,  $\bar{I}_m^{(d)}$  is suppressed and even approaches zero for  $\omega \rightarrow -1$ . Only points with  $P^2(y) = 1$  (e.g., at  $y = y_0$ ) have a finite non-zero limit, which is

$$-y_0^{d/2+1} r'_{\text{Litim}}(y_0) = y_0^{d/2-1}. \quad (37)$$

This behavior is illustrated in Fig. 2, where we show  $\bar{I}_1^{(d)}$  for  $\omega = -0.9999$  for various regulators. In the limit

$\omega \rightarrow -1$ , the area under the curve defined by the integrand associated with the threshold function obtained with the Litim regulator indeed exceeds the one of any other regulator shown in Fig. 2.

In Fig. 2, we also observe the dependence of the order relation  $\mathcal{R}$  on the number of spacetime dimensions. In order to maximize the area under the curve defined by the integrand of the threshold function,  $y_0$  should be close to  $y = 1$  for  $d > 2$  and close to  $y = 0$  for  $d < 2$ , see Fig. 2. Furthermore, if the regulator “lies” closer to the line  $P^2(y) = 1$  at  $y_0$ , e.g.,  $\partial_y^2 P^2(y)|_{y=y_0} \approx 0$ , the area under the curve defined by the integrand increases. Comparing the areas associated with various regulators and thus the strength of the singular behavior for  $\omega \rightarrow -1$ , we deduce from Fig. 2 for  $d = 4$  that

$$\begin{aligned} r_{\text{Litim}}(y) &> r_{\text{SL}}(y) > r_{\text{NSL}}(y) \\ &> r_{\text{mexp}}(y) > r_{\text{css}}(y) > r_{\text{exp2}}(y). \end{aligned} \quad (38)$$

In Fig. 2, we also observe that, with decreasing number of spacetime dimensions, the area under the curve defined by the integrand  $\bar{I}_m^{(d)}$  increases.<sup>7</sup>

In general, we conclude that, for normalized regulators, every point  $y_0$  with

$$y_0 \in \mathcal{C} := \{y \in [0, \infty) \mid P^2(y) = 1\} \quad (39)$$

generates a peak in the auxiliary function  $\bar{I}_m^{(d)}$  with the height

$$-y_0^{d/2+1} r'(y_0) \quad (40)$$

for  $\omega \rightarrow -1$ . In the following we shall refer to elements in  $\mathcal{C}$  as *contact points*. For regulators with a finite set  $\mathcal{C}$ , the auxiliary function

$$\bar{l}_m^{(d)}(\omega) = \int_0^\infty dy \bar{I}_m^{(d)}(\omega, r(y), r'(y), y), \quad (41)$$

which is directly related to the threshold function  $l_m^{(d)}(\omega)$  via Eq. (36), tends to zero for  $\omega \rightarrow -1$ .<sup>8</sup> To obtain a non-zero, finite limit, it is therefore necessary to use a regulator with an infinite set  $\mathcal{C}$ . A maximization of the area under the curve  $\bar{I}_m^{(d)}$  and thus an increase of the strength of the singular behavior of the threshold function  $l_m^{(d)}(\omega)$  close to  $\omega = -1$  can be achieved by increasing the set  $\mathcal{C}$ . Apparently, according to our definition, *stable* regulators should be those which have a large set  $\mathcal{C}$  or even an *infinite* set  $\mathcal{C}$  such as the Litim regulator.

<sup>7</sup> Loosely speaking, this behavior of the integrand tends to counteract the formation of a nontrivial ground state of the potential, as associated with spontaneous symmetry breaking. However, as we shall discuss in Sec. IV, this is not the reason for the absence of spontaneous symmetry breaking in low dimensions, i.e.,  $d < 2$ , as the latter is a regularization-independent statement [32–34].

<sup>8</sup> Note that even if  $\bar{l}_m^{(d)}$  vanishes for  $\omega \rightarrow -1$ ,  $l_m^{(d)}$  can still diverge in this limit.

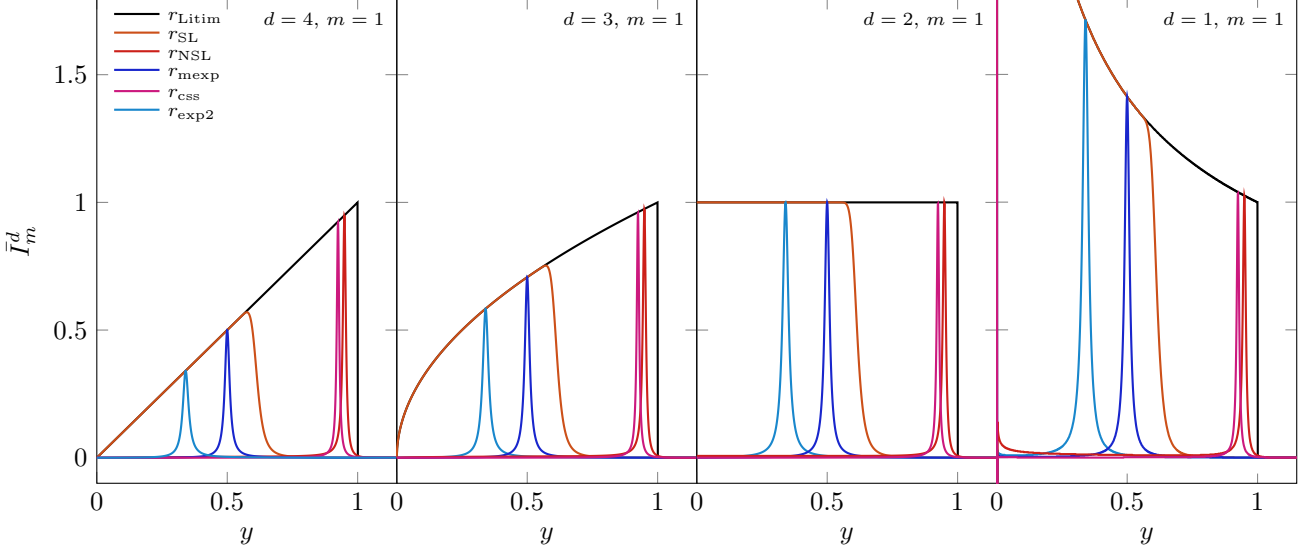


FIG. 2. The auxiliary function  $\bar{l}_m^{(d)}$  for  $m = 1$  at  $\omega = -0.9999$  for different numbers of spacetime dimensions  $d$ . For a definition of the various regulators, see Tab. I.

We would like to emphasize that, with the order relation (20) at hand, it directly follows that, in LPA, the Litim regulator is the *unique optimal* regulator in  $\mathcal{A}$  with respect to POSS since  $\mathcal{C} = [0, 1]$  and  $r' \leq 0$ . Thus, in LPA, POSS uniquely singles out the same optimal regulator as the functional optimization discussed in Ref. [13]. If we consider regulators in  $\mathcal{A}'$ , an optimal regulator  $r_{\text{opt}}$  with respect to POSS has to fulfill:

$$\bar{l}_1^{(d)}(\omega = -1, r_{\text{opt}}) = \max_{r \in \mathcal{A}'} \bar{l}_1^{(d)}(\omega = -1, r). \quad (42)$$

### C. Examples of regulators

The Principle of Strongest Singularity is not only useful to order and compare existing regulators, it also provides us with an intuitive prescription to construct *new* regulators which allow to obtain (numerically) stable RG flows. We now aim at such a construction for studies in LPA. In the first part of this subsection we shall focus on the construction of regulators in the set  $\mathcal{A}$  which are *differentiable* but still come with a singularity strength comparable to the one of the Litim regulator. The second part then deals with regulators in the set  $\mathcal{A}'$ . The singular behavior of the regulators in this set can even be stronger than the one of the Litim regulator as we shall show by an explicit construction of such a regulator.

As already discussed above, the Litim regulator is the unique optimal regulator in  $\mathcal{A}$  with respect to POSS. Therefore, it represents the natural starting point for the construction of new (at least “almost optimal”) differentiable regulators. For example, if we would like to have a differentiable Litim-like regulator, we may be tempted to replace the Heaviside function in the definition of the

Litim regulator (28) by a “smeared-out” version of it, e.g.,  $\theta(x) \approx \frac{1}{2}(1 + \tanh(\epsilon x))$  with some large value of  $\epsilon$ , e.g.,  $\epsilon = 10$ , yielding the naively smeared Litim (NSL) regulator,

$$r_{\text{NSL}}(y) = \left( \frac{1}{y} - 1 \right) \left( \frac{1}{2} \tanh(\epsilon(1-y)) + \frac{1}{2} \right). \quad (43)$$

However, after a normalization of this regulator according to Eq. (18), it then turns out that it has only one contact point,  $\mathcal{C} = \{y_0\}$ . This implies that the resulting threshold function only exhibits a weak singular behavior at  $\omega = -1$  as illustrated in Fig. 2. Hence, this simple “smeared-out version” of the Litim regulator  $r_{\text{NSL}}(y)$  is far from being a good choice with respect to POSS. Note also that  $r_{\text{NSL}}$  is not even contained in  $\mathcal{A}$  since it enters the yellow shaded region in Fig. 1.

A smooth Litim-like (SL) regulator with an infinite set  $\mathcal{C}$  is given by, e.g.,

$$r_{\text{SL}}(y) = \exp\left(-\frac{1}{y - \frac{1}{2}}\right) \theta\left(y - \frac{1}{2}\right) + \frac{1}{y} - 1, \quad (44)$$

which yields

$$P_{\text{SL}}^2(y) = y \exp\left(-\frac{1}{y - \frac{1}{2}}\right) \theta\left(y - \frac{1}{2}\right) + 1, \quad (45)$$

see Fig. 2 for an illustration.<sup>9</sup>

<sup>9</sup> Before employing the regulator (44) in a specific study, it is required to ensure that this regulator also fulfills the corresponding requirements detailed in Appendix A.

At first glance, the regulator (44) appears to be very similar to the compactly supported smooth (CSS) regulator shape functions introduced in Ref. [31], see Tab. I for the definition of the corresponding shape function  $r_{\text{css}}(y)$ . For concrete applications of this class of regulators, we refer the reader to Refs. [35–37]. However, these regulators are constructed such that  $r(y) \neq 0$  for a compactly supported region which is not the case for the regulator in Eq. (44). In fact, the regulators constructed in Ref. [31] have only one contact point,  $\mathcal{C} = \{y_0\}$  (see Fig. 1), and are therefore unstable in the spirit of POSS.

Given the fact that the regulator (44) comes with an infinite set  $\mathcal{C}$  (see Fig. 1), this regulator represents a reasonable starting point for the construction of other new regulators which are infinitely differentiable on the full domain and even close to the Litim regulator with respect to POSS. Such regulators may potentially then also turn out to be useful for studies beyond LPA where differentiability of regulators in general becomes a crucial property at some point. Furthermore, it is in principle also possible to construct regulators which combine the properties of the ones associated with the shape functions  $r_{\text{SL}}(y)$  and  $r_{\text{css}}(y)$ , i.e., compactly supported smooth regulator shape functions which approach the Litim regulator at a nonzero  $y$ .<sup>10</sup> Such a combination may be useful for studies beyond LPA, i.e., at high(er) orders of the derivative expansion of the effective action, where, e.g., the Litim regulator is no longer optimal in the spirit of functional optimization [13] and, depending on the order of the derivative expansion, not even applicable because of the lack of differentiability.

As a second application of POSS, we construct a regulator whose singular behavior even exceeds the one of the Litim regulator. Clearly, this is not possible within the set  $\mathcal{A}$  since, in LPA, the Litim regulator is the unique optimal regulator in  $\mathcal{A}$  with respect to POSS. Therefore, we have to consider the set  $\mathcal{A}' \setminus \mathcal{A}$ .<sup>11</sup> A simple initial guess for such a regulator with a strong divergent (SD) behavior may be

$$r_{\text{SD}}(y) = \begin{cases} \frac{1}{y} - 1 & (0 \leq y < y_0) \\ \frac{s(y-y_0)+1}{y} - 1 & (y_0 \leq y < \frac{1-sy_0}{1-s}) \\ 0 & (\frac{1-sy_0}{1-s} \leq y) \end{cases}, \quad (46)$$

<sup>10</sup> More precisely, we may construct a smooth regulator with  $P^2(y) = 1$  for  $0 \leq y < y_0$  and  $P^2(y) = y$  for  $y_1 \leq y$ . The intermediate region,  $y_0 \leq y < y_1$  can then be bridged by a smooth function which smoothly connects to the functions in the other regions. It may be chosen to be of, e.g., the following form:

$$\begin{aligned} P^2(y) = & y \exp \left\{ -a \exp \left\{ \frac{1}{y-y_0} + \frac{1}{y-y_1} \right\} \right\} \\ & - \exp \left\{ - \exp \left\{ \frac{1}{y-y_0} + \frac{1}{y-y_1} \right\} \right\} + 1, \end{aligned}$$

where  $y_0 = 0.5$ ,  $y_1 = 1.5$  and  $a = 0.625$ .

<sup>11</sup> It would be interesting to include regulators from the set  $\mathcal{A}' \setminus \mathcal{A}$  into an analysis based on functional optimization as discussed in Ref. [13].

which yields

$$P_{\text{SD}}^2(y) = \begin{cases} 1 & (0 \leq y < y_0) \\ s(y - y_0) + 1 & (y_0 \leq y < \frac{1-sy_0}{1-s}) \\ y & (\frac{1-sy_0}{1-s} \leq y) \end{cases}.$$

Here,  $y_0 > 1$  denotes the width of the interval  $\mathcal{C} = [0, y_0]$  and  $s > 1$  is the slope of the linear connection line between  $P^2(y = y_0) = 1$  and the point  $y = (1-sy_0)/(1-s)$  above which we have  $P^2(y) = y$ . The parameters  $s$  and  $y_0$  are constrained by the fact that we are requiring the threshold functions to be positive. Note that the regulator assumes negative values between  $y = 1$  and  $y = (1-sy_0)/(1-s)$ , i.e., it enters the yellow shaded region in Fig. 1. In  $d = 4$ , we find an upper bound for  $y_0$ , which is  $y_0 < 3/2$ . For any such  $y_0$ , a lower bound for  $s$  exists such that the threshold functions in LPA remain positive. For example, in  $d = 4$ , we may choose  $y_0 = 1.3$  and  $s = 1.7$ . Note that the simple structure of this regulator in principle allows for an analytic computation of the threshold functions.

#### IV. STABILITY OF RG FLOWS

In order to illustrate that POSS is indeed useful for the construction of regulators which generate (numerically) stable RG flows, we consider again the RG flow equation (15) for the effective potential  $U_k$  of a scalar field theory in  $d = 4$  spacetime dimensions in LPA for various regulators. To be specific, we consider several regulators including the standard Litim regulator ( $r_{\text{Litim}}$ ), the naively “smeared-out” Litim regulator ( $r_{\text{NSL}}$ ), a compactly supported smooth regulator ( $r_{\text{css}}$ ), two variants of exponential regulators ( $r_{\text{exp2}}$  and  $r_{\text{mexp}}$ ), the smooth regulator ( $r_{\text{SL}}$ ) introduced in Eq. (44), and the SD regulator ( $r_{\text{SD}}$ ) introduced in Eq. (46) associated with a particularly strong singular behavior close to  $\omega = -1$ , see also Tab. I for the definitions of these regulators. Moreover, in order to demonstrate explicitly the relation between the stability of the RG flows and the set  $\mathcal{C}$  of a given regulator,<sup>12</sup> we add yet another family of regulators:

$$r_{x_0}(y) = \frac{((1-x_0)e^{x_0-y} + y-1)\theta(y-x_0) + 1}{y} - 1. \quad (47)$$

This regulator family can be adjusted by choosing  $x_0 \in [0, 1]$ . For  $y \in [0, x_0]$ , we have  $P^2(y) = 1$  and, for  $y \in [x_0, \infty]$ , we find that  $P^2(y)$  approaches the asymptote  $y$  exponentially. For  $x_0 = 1$ , we find  $r_{x_0}(y) = r_{\text{Litim}}(y)$ . Thus, by adjusting  $x_0$ , we can continuously vary the set  $\mathcal{C}$  which implies a variation of the strength of the singular

<sup>12</sup> Recall that the set  $\mathcal{C}$  contains all points of contact of a given regulator with  $P^2(y) = 1$ , see Eq. (39).

behavior of the threshold function. Moreover, to illustrate the effect of having more than one but still a finite number of global minima of  $P^2(y)$ , we introduce an oscillatory regulator ( $r_{\text{osc}}$ ):

$$r_{\text{osc}}(y) = \theta(1-y)(A(1-\cos(2\pi ny)) - y + 1) + y, \quad (48)$$

where  $n = |\mathcal{C}| - 1$  and  $A < 1/(2\pi n(1 - \frac{3}{4n}) - 1)$  such that  $r'_{\text{osc}}(y) \leq 0$ . For concreteness, we shall use  $A \approx 0.0157$  and  $n = 10$  in our numerical studies below. Note that  $r_{\text{osc}}$  as well as the regulator family  $r_{x_0}$  do not fall in the class of differentiable regulators.

For the regulators considered in this section, POSS predicts the following regulator hierarchy for LPA in  $d = 4$  spacetime dimensions:

$$\begin{aligned} r_{\text{SD}}(y) &> r_{\text{Litim}}(y) > r_{x_0=0.8}(y) > r_{\text{SL}}(y) \\ &> r_{x_0=0.5}(y) > r_{x_0=0.2}(y) > r_{\text{osc}}(y) \\ &> r_{\text{NSL}}(y) > r_{\text{mexp}}(y) > r_{\text{css}}(y) > r_{\text{exp2}}(y). \end{aligned} \quad (49)$$

This follows from Fig. 3 together with Eq. (20). More precisely, for regulators with an infinite set  $\mathcal{C}$ , the auxiliary function  $\bar{l}_1^{(4)}$  approaches a finite value in the limit  $\omega \rightarrow -1$ , whereas it approaches zero for those regulators with a finite set  $\mathcal{C}$ , see Fig. 3. Note that, in accordance with POSS, we find that the oscillatory regulator  $r_{\text{osc}}$  with more than one element in  $\mathcal{C}$  is *more stable* than any of the analytic regulators with only one contact point, i.e.,  $\mathcal{C} = \{y_0\}$ . Moreover, from the standpoint of POSS, the SD regulator is *more stable* than the Litim regulator. However, we emphasize that these two regulators are associated with two different sets of regulators, namely the sets  $\mathcal{A}' \setminus \mathcal{A}$  and  $\mathcal{A}$ , respectively.

In order to solve the flow equation for the effective potential numerically, we follow Refs. [22–24, 26, 38, 39] and reformulate the RG flow equation (15) such that it resembles the form of conservation laws in fluid dynamics. To be specific, we simply take a total derivative on both sides with respect to  $\phi$  and introduce the slope  $u_k(\phi) = \partial_\phi U_k(\phi)$  of the effective potential with respect to the field  $\phi$  as a new variable. The flow equation for the latter quantity then reads

$$\begin{aligned} \partial_t u_k(\phi) &= \frac{d}{d\phi} \left( -\frac{1}{2} \frac{\text{surf}(d)k^d}{(2\pi)^d} l_1^{(d)}(\omega) \right) \\ &= \frac{1}{2} \frac{\text{surf}(d)k^{d-2}}{(2\pi)^d} l_2^{(d)}(\omega) \partial_\phi^2 u_k(\phi). \end{aligned} \quad (50)$$

This flow equation can be viewed as a non-linear diffusion equation, where

$$\alpha_k(\omega) = \frac{1}{2} \frac{\text{surf}(d)k^{d-2}}{(2\pi)^d} l_2^{(d)}(\omega) \geq 0 \quad (51)$$

is the diffusion coefficient.

The flow equation (50) can now be solved with methods borrowed from numerical fluid dynamics [24, 26] without relying on a specific ansatz for the effective potential.

As numerical method for the solution of the RG flow equation (50), we employ the Kurganov-Tadmor (KT) scheme [40]. This is a finite-volume method which has already been tested and used to solve such equations, see, e.g., Ref. [25].<sup>13</sup> Note that a negative diffusion coefficient (51) would lead to backwards diffusion which causes numerical instabilities at least within our numerical treatment.

Since we are interested in studying situations where the ground state of the theory is governed by spontaneous symmetry breaking in the IR limit, we briefly discuss the associated emergence of a nontrivial minimum in the effective potential by examining the flow equation (50). From this equation, we deduce that spontaneous symmetry breaking can only appear if the slope  $u_k(\phi)$  of the effective potential  $U_k(\phi)$  with respect to  $\phi$  splits up into two distinct regions, separated by an “insulating point”  $\phi_0$  with  $\phi_0^2 > 0$ . This insulating point is defined by  $\omega = \partial_\phi u_k(\phi = \phi_0)/k^2 = 0$ .<sup>14</sup> At this point, the diffusion coefficient  $\alpha_k(0)$  vanishes in the IR limit. For example, in  $d > 2$ , the diffusion coefficient vanishes for  $k \rightarrow 0$ , since  $l_2^{(2)}(0)$  is a constant and thus

$$\alpha_k(0) \propto k^{(d-2)}. \quad (52)$$

Hence, for  $d > 2$ , it is at least in principle possible to encounter spontaneous symmetry breaking in the IR limit. On the other hand, for  $d < 2$ ,  $\phi_0$  is always affected by a non-vanishing diffusion coefficient such that it cannot be an insulating point and therefore the dynamics of bosons as described by our scalar field tends to restore the symmetry in the IR limit.

Let us now assume that a finite insulating point  $\phi_0$  exists in the IR limit. In the region  $\phi^2 < \phi_0^2$ , where the slope of  $u_k(\phi)$  is negative (i.e.,  $\omega < 0$ ), the diffusion coefficient becomes much greater than in the region  $\phi^2 > \phi_0^2$  (i.e.,  $\omega > 0$ ) at sufficiently small RG scales, since every point inside the region  $\phi^2 < \phi_0^2$  is “pushed” into the singularity associated with  $\omega = -1$ . As a consequence, this region becomes flat and does not contain any physical information in the limit  $k \rightarrow 0$ .

For the RG flow equation (50) with  $d = 4$ , a finite insulating point potentially exists for certain classes of initial conditions at the scale  $k = \Lambda$ , e.g.,

$$U_\Lambda(\phi) = \frac{1}{2} m^2 \phi^2 + \frac{1}{4} \lambda \phi^4 \quad (53)$$

with  $m^2 < 0$  and  $\lambda > 0$ . In the following, we set  $\lambda = 1.0$  for all regulators. The parameter  $m^2 < 0$  is tuned such

<sup>13</sup> The precise implementation of the KT scheme in the context of functional RG equations used in the present work can be found in Refs. [24, 29]. For a meaningful comparison of the RG flows with different regulators, we employed the same numerical control parameters:  $\phi_{\text{max}} = 1.5\Lambda$ ,  $\Delta\phi = 0.001\Lambda$ , for all regulators. As numerical time stepper we used `solve_ivp` [41] with “LSODA” with  $rtol = atol = 10^{-10}$  for its relative and absolute error.

<sup>14</sup> Note that  $\phi_0$  should not be confused with the minimum of the effective potential.

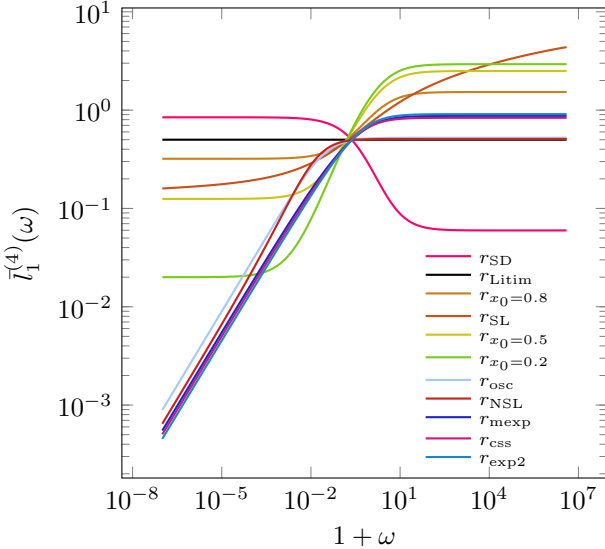


FIG. 3. Dependence of the auxiliary function  $\bar{l}_1^{(4)}$  on the mass parameter  $\omega$ . The definition of this function, which is directly related to the threshold function  $l_1^{(4)}$ , can be found in Eq. (41). Note that any regulator with an infinite set  $\mathcal{C}$  approaches a nonzero value for  $\omega \rightarrow -1$ . From the  $\omega$ -dependence of these functions and the order relation (20), we can extract the hierarchy of regulators given in Eq. (49).

that we obtain  $\phi_{\min}/\Lambda = 0.3$  for the position of the minimum of the effective potential at the scale at which the RG flow breaks down numerically for a given regulator.<sup>15</sup> In this way, we ensure that our comparison of the stability of RG flows resulting from different regulators is at least to some extent meaningful. Of course, ideally, such a comparison would require to tune the initial conditions such that the effective potential  $U_k$  is identical for  $k \rightarrow 0$  for all regulators. However, this is impossible as all RG flows eventually break down at a finite RG scale in our present numerical setup due to limited precision of the time stepper.<sup>16</sup>

<sup>15</sup> Note that the (initial) values for  $m^2/\Lambda^2$  depend only mildly on the regulators considered in the present work. To be more specific, we find  $m^2/\Lambda^2 \in [-0.099, -0.093]$ .

<sup>16</sup> Note that, as discussed in Ref. [42], the RG flow equation for the effective potential can be reformulated to circumvent the issue of a numerical breakdown at a finite RG scale. At least for a certain class of regulators, this suggests that it is possible to find a reformulation of the flow equation or an improvement of the numerical solver which potentially allows to follow the RG flow down to very small RG scales where the potential eventually becomes flat. However, our present work focuses on the construction of regulators leading to a fast flattening of the effective potential in terms of RG time which we demonstrate with a fixed numerical setup. Such a fast flattening of the effective potential essentially introduces a natural stabilization of RG flows as discussed above. In any case, a combination of the reformulation presented in Ref. [42] with regulators considered optimal according to our definition would be interesting but is beyond the scope of the present study.

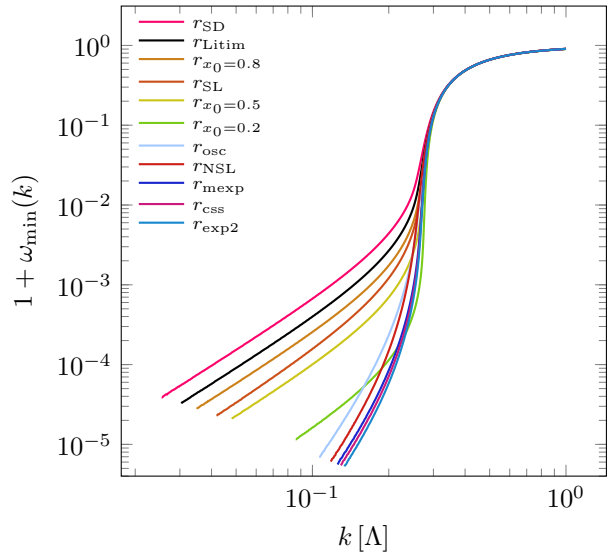


FIG. 4. The quantity  $\omega_{\min}(k)$  as obtained from various regulators as a function of the RG scale  $k$ , down to the scale where the numerical calculations break down for a given regulator. The ordering of these breakdown scales correspond to the regulator hierarchy predicted by POSS, see Eq. (49) and also Fig. 3. Note that, at a fixed RG scale  $k$ , a larger  $\omega_{\min}$  corresponds to a flatter potential. This implies that, in terms of RG time, the effective potential becomes flat faster for regulators which are considered to be preferred according to POSS. The derivative of the effective potential,  $u_k(\phi) = \partial_\phi U_k(\phi)$ , at the different (numerical) breakdown scales is shown in Fig. 5.

In order to illustrate that the hierarchy of regulators (49) indeed provides us with a *good* measure for the stability of RG flows, we solve the flow equation (50) for the different regulators and extract  $\omega_{\min}(k)$ , which is defined to be the smallest value of  $\omega$  at a given RG scale  $k$ . This quantity then allows us to illustrate how fast (in terms of the RG time  $t$ ) the RG flow approaches the singularity.

For the regulators considered in this work,  $\omega_{\min}$  is shown in Fig. 4. We observe that, at a fixed, sufficiently small RG scale, the values of  $\omega_{\min}$  follow identically the regulator hierarchy predicted by POSS, see Eq. (49): More stable RG flows yield flatter potentials, which is a direct consequence of the self-healing property. Consequently, less stable RG flows approach the singularity at  $\omega = \omega_{\text{pole}} = -1$  faster in terms of the RG time  $t$  and eventually break down earlier due to the limited numerical precision, in accordance with our definition of numerical stability. Also, the ordering of the breakdown scales associated with the various RG flows is in perfect agreement with the predicted regulator hierarchy as given in Eq. (49). As it should be, this ordering is also visible in Fig. 5, where we show the slope  $u_k(\phi)$  of the effective potential at the numerical breakdown scale

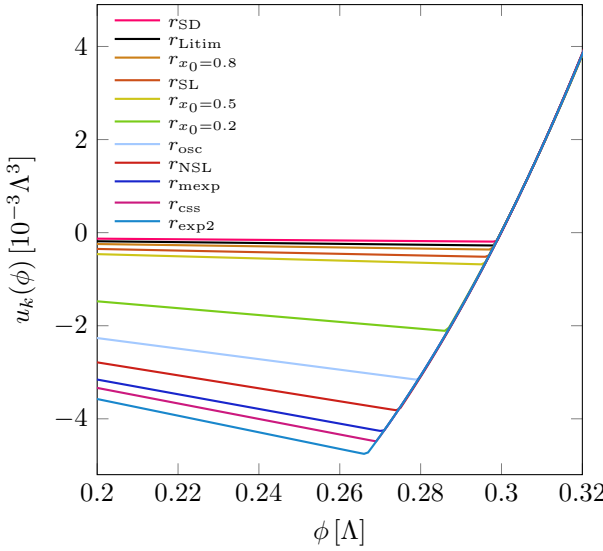


FIG. 5. Derivative of the effective potential,  $u_k(\phi) = \partial_\phi U_k(\phi)$ , as a function of  $\phi$  for various regulators at the scale  $k_{\text{break}}$ , where the RG flow breaks down. The UV potentials of the RG flows associated with the various regulators are tuned such that the position  $\phi_{\min}$  of the minimum of the effective potential is the same for all regulators at the respective scale  $k_{\text{break}}$ , i.e.,  $\phi_{\min}/\Lambda = 0.3$ . Note that the position of the minimum of the potential is associated with the position of the zero of the depicted derivative of the effective potential,  $u_k(\phi)$ . We observe that the hierarchy of regulators predicted by POSS is in accordance with the observed “flatness” of the effective potentials indicated by a small/vanishing derivative  $u_k(\phi)$ , see also Eq. (49).

for the regulators considered in our analysis.<sup>17</sup>

Comparing the RG flows obtained from the various regulators, we observe that the values of the smallest RG scale, which is numerically accessible for a given regulator, differ significantly. In fact, the breakdown scales for regulators with only one element in  $\mathcal{C}$  are a factor of 5 – 10 times greater than the scales that can be reached with regulators with an infinite set  $\mathcal{C}$ .

In summary, our analysis provides a quantitative confirmation that the (numerical) stability of RG flows can indeed be improved by a suitable choice of the regulator. POSS allows to single out regulators which generate (numerically) stable RG flows. Such regulators allow to access the deep infrared regime, where the potential becomes convex. From a phenomenological standpoint, the access to this regime is ultimately required for quantitative studies of critical behavior in the presence of a

(small) explicit symmetry breaking [43] and the computation of the corresponding scaling functions, as done in, e.g., Ref. [44]. For such studies, the use of regulators with an infinite set of contact points appears inevitable.

## V. CONCLUSIONS

In this work, we discussed the optimization of functional RG flows from the standpoint of stability which is tightly connected to the presence of zeroes in the spectrum of the regularized two-point function. In fact, the inverse of the regularized two-point function determines the RG flow of the effective action and therefore the zero eigenvalues of the regularized two-point function define singular points which control how fast (measured in terms of RG time) the effective potential becomes convex, in particular in situations where the dynamics of a theory is governed by spontaneous symmetry breaking.

We discussed that the stability in numerical calculations can indeed be considerably improved by a suitable choice of the regulator. Of course, such a stability analysis requires to compare different RG flows which, within a given truncation, corresponds to comparing different regulators. To render such a comparison meaningful, we introduced a comparability condition and a corresponding principle, the Principle of Strongest Singularity, which provides us with an order relation for regulator functions.

We demonstrated the application of this general principle by using the example of a scalar field theory in LPA. In LPA, the comparability condition can be viewed as a normalization condition for regulator functions. The order relation becomes independent of the RG flow in this approximation but it depends on the number of space-time dimensions. Within this analysis, we also provided an intuitive picture of how the behavior of RG flows close to the aforementioned singular points is related to properties of the threshold functions.

For RG flows in LPA, we find that the Litim regulator provides the strongest singular behavior and is therefore the unique optimal regulator according to POSS, at least within the standard set of regulator functions considered in the context of functional RG studies. This implies that, in LPA, the well-known functional optimization [13] and POSS single out the same regulator as optimal: That is the Litim regulator. Moreover, we constructed a regulator which is close to the Litim regulator with respect to POSS but is differentiable. In general, our analysis clearly indicates that analytic regulators generate significantly less stable RG flows than the Litim regulator. In addition, by extending the set of functions associated with the standard regulators, we found that we can even construct regulators which come with a stronger singular behavior than the one exhibited by the Litim regulator and therefore generate particularly stable RG flows in the spirit of POSS.

We close by emphasizing that POSS does *a priori* not entail a minimization of the regulator dependence of

<sup>17</sup> The numerical stability as well as the potentials at the breakdown scale presented in Fig. 5 do not rely on the normalization condition (18), since the (abstract) RG trajectory is not affected by a rescaling and hence the numerical solver will break down at the same infrared potential.

physical observables. In other words, it is not apparent that functional optimization and POSS in general single out the same regulator(s). Therefore, a natural extension of our analysis represents the computation of, e.g., critical exponents with regulators considered to be *good* according to POSS, in particular with those characterized by a particularly strong singular behavior. Moreover, an analysis of how fast physical observables converge in the RG flow may be interesting as this should be solely encoded in the dependence of the threshold functions on the mass parameter which is determined by the regulator, see Fig. 3. In any case, given our analysis in LPA, where the Litim regulator is singled out by both optimization criteria (within the standard set of regulator functions), it appears at least reasonable to expect that, beyond LPA, the application of both criteria may also yield a set of regulator functions which may be simultaneously classified as “good regulators”, i.e., regulators which yield stable RG flows according to POSS and are associated with a “short” trajectory in theory space according to the definition in Ref. [13]. Smooth regulators, which are singled out in LPA by POSS, may represent a good starting point for the construction of such regulators for computations of the effective action at higher orders of the derivative expansion.

## ACKNOWLEDGMENTS

We thank A. Gei  el, A. K  nigstein, J. M. Pawlowski, M. J. Steil, and N. Wink for useful discussions and comments on the manuscript. J.B. acknowledges support by the DFG under grant BR 4005/4-1 and BR 4005/6-1 (Heisenberg program). As members of the fQCD collaboration [45], the authors also would like to thank the other members of this collaboration for discussions. Moreover, this work is supported by the *Deutsche Forschungsgemeinschaft* (DFG, German Research Foundation) through the CRC-TR 211 “Strong-interaction matter under extreme conditions” – project number 315477589 – TRR 211 and by the State of Hesse within the Research Cluster ELEMENTS (Project No. 500/10.006). All numerical results as well as all figures in this work have been obtained by using *Python 3* [46] with various libraries [41, 47, 48], if not explicitly stated otherwise. Some of the results have been cross-checked with *Mathematica* [49].

## Appendix A: Constraints for regulator functions

For the following discussion of constraints for the regulator, we focus on threshold functions as they appear in LPA. It then follows that a general regulator shape function  $r$  should render the threshold functions appearing in the flow equations finite for  $\omega > -\min_y P^2(y)$ . Moreover, the threshold functions should diverge at  $\omega = -\min_y P^2(y)$ , see our discussion in Subsec. II B. In gen-

eral, the standard constraints detailed in Eq. (24) or, equivalently, in Eq. (25) are not sufficient in this respect. Hence, it is necessary to identify additional constraints which supplement the standard constraints for regulator shape functions. As we shall discuss below, these additional constraints in general depend on, e.g., the number of spacetime dimensions  $d$  and on the position of the poles of the integrand associated with the threshold functions.

In the following we shall assume that the regulator shape function and its derivative behave as  $r(y) \sim y^{-\alpha}$  and  $r'(y) \sim y^{-\alpha-1}$  in the limits  $y \rightarrow 0$  and  $y \rightarrow \infty$ , respectively. Constraints for the parameter  $\alpha$  are derived below. For concreteness, we use the normalization (18), i.e.,  $\min_y P^2(y) = 1$ . However, the following analysis does not rely on this normalization.

Let us begin by discussing the issue of finiteness of the threshold functions, i.e., we first consider  $\omega > -1$ . In the limit  $y \rightarrow \infty$ , the integrand (14) of the threshold function (13) then becomes independent of  $\omega$  since  $P^2(y)$  dominates the denominator:

$$I_m^{(d)}(\omega, \dots) \sim y^{d/2+1} \frac{y^{-\alpha-1}}{y^m} \text{ for } y \rightarrow \infty. \quad (\text{A1})$$

Consequently, for  $y \gg 1$ , it is required that

$$-\alpha < -1 - \frac{d}{2} + m \quad (\text{A2})$$

to render the threshold functions finite. Recall that the parameter  $m$  counts the number of internal lines of the 1PI diagram associated with the threshold function (13).

In the limit  $y \rightarrow 0$  and  $\omega > -1$ , we have to distinguish between two cases:

(i)  $\lim_{y \rightarrow 0} P^2(y) < \infty$ , i.e.,  $\alpha = 1$ . For  $\omega > -1$ , we find

$$I_m^{(d)} \sim c_m(y, \omega) y^{d/2+1} y^{-\alpha-1} \text{ for } y \rightarrow 0, \quad (\text{A3})$$

where  $c_m(y, \omega)$  depends on  $\omega$  and on  $y$  but is finite for  $\omega > -1$ :

$$c_m(y, \omega) = \frac{1}{(P^2(y) + \omega)^m}. \quad (\text{A4})$$

Finiteness of the threshold function only requires  $d > 0$ . Note that the integrand  $I_m^{(d)}$  is nevertheless divergent for  $d < 2$ , see also Fig. 2.

(ii)  $\lim_{y \rightarrow 0} P^2(y) = \infty$ , i.e.,  $\alpha > 1$ . In this case,  $\omega$  can be ignored, i.e.,

$$P^2(y) + \omega \approx P^2(y) \quad (\text{A5})$$

for  $y \rightarrow 0$ . We then find

$$I_m^{(d)} \sim y^{d/2+1} \frac{y^{-\alpha-1}}{y^{m-\alpha m}} \text{ for } y \rightarrow 0. \quad (\text{A6})$$

Consequently, it is required that

$$-\alpha > -1 - d/2 + m - m\alpha \quad (\text{A7})$$

to render the threshold functions finite. Note that, in this case,  $y_0$  assumes a finite value. Recall that  $y_0$  is defined by  $P^2(y = y_0) = 1$ , see also the discussion of Eq. (29).

Next, we turn to an analysis of the behavior of the threshold functions for  $\omega \rightarrow -1$ . In this limit, the threshold functions exhibit a singular behavior, if  $m \geq 1/2$  and if the pole of the integrand is located at a finite value  $y_0$ , i.e.,  $y_0 > 0$  with  $P^2(y = y_0) = 1$ . In the following this is illustrated for analytic regulator shape functions with only one nonzero  $y_0$ . With Eqs. (31) to (33), we find for such regulators that

$$\begin{aligned} I_m^{(d)}(\omega, r(y), r'(y), y) &> -y^{\frac{d}{2}+1} \frac{\partial_y r_{\text{Litim}}(y)}{(P^2(y) + \omega)^m} \quad (\text{A8}) \\ &= \frac{y^{\frac{d}{2}-1}}{(P^2(y) + \omega)^m} \end{aligned}$$

for  $y < y_0$ . By performing now a Taylor expansion of  $P^2(y)$  about  $y_0$ , we find for some fixed  $\delta > 0$  that the integral

$$\int_{y_0-\delta}^{y_0} dy \frac{y^{\frac{d}{2}-1}}{\left(\frac{1}{2}\partial_y^2 P^2(y=y_0)(y-y_0)^2 + 1 + \omega\right)^m}$$

diverges for  $m \geq 1/2$  and  $d > 0$  in the limit  $\omega \rightarrow -1$ . Consequently,  $l_m^{(d)}(\omega)$  diverges in this limit. However, if

$y_0 = 0$  is the only contact point (i.e.,  $r(y) \sim 1/y$ ), we have  $c_m(y, \omega) \sim 1/y^m$  in Eq. (A3) at  $\omega = -1$  for  $y \rightarrow 0$ . Hence, the integral does not diverge in the limit  $\omega \rightarrow -1$ , at least for  $d/2 > m$ . For example, the standard exponential regulator  $r_{\text{exp}}(y) = 1/(\exp(y) - 1)$  (see Fig. 1) yields a global minimum of  $P^2(y)$  at  $y_0 = 0$  and therefore the threshold function  $l_m^{(d)}$  with  $m = 1$  does not diverge at  $\omega = -1$  for  $d > 2$  in this case, see also Ref. [30]. According to POSS and our corresponding numerical analysis presented in the main text, this class of regulators in general generates (numerically) unstable RG flows in situations where the ground state is governed by spontaneous symmetry breaking, at least in studies where the full field dependence of the potential is considered.

We close our analysis by noting that neither the finiteness of the threshold functions for  $\omega > -1$  nor the presence of a divergence in the limit  $\omega \rightarrow -1$  follow necessarily from the constraints (24) for general regulator shape functions. For example, according to our analysis and POSS, suitable general purpose regulators in all dimensions  $d > 0$  and for all  $m \geq 1/2$  are those which diverge as  $1/y$  for  $y \rightarrow 0$ , approach zero in the limit  $y \rightarrow \infty$  faster than  $y^{-d/2-1}$  and yield an integrand of the threshold functions with at least one nonzero pole position  $y_0$ .

---

[1] P. M. Stevenson, Optimized Perturbation Theory, *Phys. Rev. D* **23**, 2916 (1981).

[2] C. Wetterich, Exact evolution equation for the effective potential, *Phys. Lett. B* **301**, 90 (1993), arXiv:1710.05815 [hep-th].

[3] S.-B. Liao, J. Polonyi, and M. Strickland, Optimization of renormalization group flow, *Nucl. Phys. B* **567**, 493 (2000), arXiv:hep-th/9905206.

[4] L. Canet, B. Delamotte, D. Mouhanna, and J. Vidal, Optimization of the derivative expansion in the nonperturbative renormalization group, *Phys. Rev. D* **67**, 065004 (2003), arXiv:hep-th/0211055.

[5] L. Canet, B. Delamotte, D. Mouhanna, and J. Vidal, Nonperturbative renormalization group approach to the Ising model: A Derivative expansion at order partial\*\*4, *Phys. Rev. B* **68**, 064421 (2003), arXiv:hep-th/0302227.

[6] I. Balog, H. Chaté, B. Delamotte, M. Marohnic, and N. Wschebor, Convergence of Nonperturbative Approximations to the Renormalization Group, *Phys. Rev. Lett.* **123**, 240604 (2019), arXiv:1907.01829 [cond-mat.stat-mech].

[7] G. De Polsi, I. Balog, M. Tissier, and N. Wschebor, Precision calculation of critical exponents in the  $O(N)$  universality classes with the nonperturbative renormalization group, *Phys. Rev. E* **101**, 042113 (2020), arXiv:2001.07525 [cond-mat.stat-mech].

[8] G. De Polsi, G. Hernández-Chifflet, and N. Wschebor, Precision calculation of universal amplitude ratios in  $O(N)$  universality classes: Derivative expansion results at order  $O(\partial 4)$ , *Phys. Rev. E* **104**, 064101 (2021), arXiv:2109.14731 [cond-mat.stat-mech].

[9] G. De Polsi and N. Wschebor, Regulator dependence in the functional renormalization group: A quantitative explanation, *Phys. Rev. E* **106**, 024111 (2022), arXiv:2204.09170 [cond-mat.stat-mech].

[10] D. F. Litim, Optimization of the exact renormalization group, *Phys. Lett. B* **486**, 92 (2000), arXiv:hep-th/0005245.

[11] D. F. Litim, Optimized renormalization group flows, *Phys. Rev. D* **64**, 105007 (2001), arXiv:hep-th/0103195.

[12] D. F. Litim, Mind the gap, *Int. J. Mod. Phys. A* **16**, 2081 (2001), arXiv:hep-th/0104221.

[13] J. M. Pawłowski, Aspects of the functional renormalisation group, *Annals Phys.* **322**, 2831 (2007), arXiv:hep-th/0512261.

[14] D. F. Litim, Critical exponents from optimized renormalization group flows, *Nucl. Phys. B* **631**, 128 (2002), arXiv:hep-th/0203006.

[15] D. F. Litim and L. Vergara, Subleading critical exponents from the renormalization group, *Phys. Lett. B* **581**, 263 (2004), arXiv:hep-th/0310101.

[16] D. F. Litim, Towards functional flows for hierarchical models, *Phys. Rev. D* **76**, 105001 (2007), arXiv:0704.1514 [hep-th].

[17] D. F. Litim and D. Zappala, Ising exponents from the functional renormalisation group, *Phys. Rev. D* **83**,

085009 (2011), arXiv:1009.1948 [hep-th].

[18] J. Braun, H. Gies, and J. M. Pawłowski, Quark Confinement from Color Confinement, *Phys. Lett. B* **684**, 262 (2010), arXiv:0708.2413 [hep-th].

[19] J. M. Pawłowski, M. M. Scherer, R. Schmidt, and S. J. Wetzel, Physics and the choice of regulators in functional renormalisation group flows, *Annals Phys.* **384**, 165 (2017), arXiv:1512.03598 [hep-th].

[20] I. Balog, G. De Polsi, M. Tissier, and N. Wschebor, Conformal invariance in the nonperturbative renormalization group: a rationale for choosing the regulator, *Phys. Rev. E* **101**, 062146 (2020), arXiv:2004.02521 [cond-mat.stat-mech].

[21] B. Delamotte, G. De Polsi, M. Tissier, and N. Wschebor, Conformal invariance and composite operators: A strategy for improving the derivative expansion of the non-perturbative renormalization group, *Phys. Rev. E* **109**, 064152 (2024), arXiv:2401.02517 [cond-mat.stat-mech].

[22] E. Grossi and N. Wink, Resolving phase transitions with Discontinuous Galerkin methods (2019), arXiv:1903.09503 [hep-th].

[23] E. Grossi, F. J. Ihssen, J. M. Pawłowski, and N. Wink, Shocks and quark-meson scatterings at large density, *Phys. Rev. D* **104**, 016028 (2021), arXiv:2102.01602 [hep-ph].

[24] A. Koenigstein, M. J. Steil, N. Wink, E. Grossi, J. Braun, M. Buballa, and D. H. Rischke, Numerical fluid dynamics for FRG flow equations: Zero-dimensional QFTs as numerical test cases. I. The  $O(N)$  model, *Phys. Rev. D* **106**, 065012 (2022), arXiv:2108.02504 [cond-mat.stat-mech].

[25] A. Koenigstein, M. J. Steil, N. Wink, E. Grossi, and J. Braun, Numerical fluid dynamics for FRG flow equations: Zero-dimensional QFTs as numerical test cases. II. Entropy production and irreversibility of RG flows, *Phys. Rev. D* **106**, 065013 (2022), arXiv:2108.10085 [cond-mat.stat-mech].

[26] A. Koenigstein, *Non-perturbative aspects of (low-dimensional) quantum field theories*, Ph.D. thesis, Goethe U., Frankfurt (Main) (2023).

[27] M. J. Steil and A. Koenigstein, Numerical fluid dynamics for FRG flow equations: Zero-dimensional QFTs as numerical test cases. III. Shock and rarefaction waves in RG flows reveal limitations of the  $N \rightarrow \infty$  limit in  $O(N)$ -type models, *Phys. Rev. D* **106**, 065014 (2022), arXiv:2108.04037 [cond-mat.stat-mech].

[28] D. F. Litim, J. M. Pawłowski, and L. Vergara, Convexity of the effective action from functional flows, arXiv:hep-th/0602140 (2006).

[29] J. Stoll, N. Zorbach, A. Koenigstein, M. J. Steil, and S. Rechenberger, Bosonic fluctuations in the  $(1+1)$ -dimensional Gross-Neveu(-Yukawa) model at varying  $\mu$  and  $T$  and finite  $N$ , arXiv:2108.10616 [hep-ph] (2021).

[30] M. Peláez and N. Wschebor, Ordered phase of the  $O(N)$  model within the nonperturbative renormalization group, *Phys. Rev. E* **94**, 042136 (2016), arXiv:1510.05709 [cond-mat.stat-mech].

[31] I. Nandori, Functional renormalization group with a compactly supported smooth regulator function, *JHEP* **04**, 150, arXiv:1208.5021 [hep-th].

[32] N. D. Mermin and H. Wagner, Absence of ferromagnetism or antiferromagnetism in one- or two-dimensional isotropic heisenberg models, *Phys. Rev. Lett.* **17**, 1133 (1966).

[33] P. C. Hohenberg, Existence of long-range order in one and two dimensions, *Phys. Rev.* **158**, 383 (1967).

[34] S. Coleman, There are no goldstone bosons in two dimensions, *Communications in Mathematical Physics* **31**, 259 (1973).

[35] I. G. Máríán, U. D. Jentschura, and I. Nandori, The numerically optimized regulator and the functional renormalization group, *J. Phys. G* **41**, 055001 (2014), arXiv:1311.7377 [hep-th].

[36] I. Nandori, I. G. Marian, and V. Bacso, Spontaneous symmetry breaking and optimization of functional renormalization group, *Phys. Rev. D* **89**, 047701 (2014), arXiv:1303.4508 [hep-th].

[37] J. Kovacs, S. Nagy, and K. Sailer, Optimized regulator for the quantized anharmonic oscillator, *Int. J. Mod. Phys. A* **30**, 1550058 (2015), arXiv:1403.3544 [hep-th].

[38] K.-I. Aoki, S.-I. Kumamoto, and D. Sato, Weak solution of the non-perturbative renormalization group equation to describe dynamical chiral symmetry breaking, *PTEP* **2014**, 043B05 (2014), arXiv:1403.0174 [hep-th].

[39] K.-I. Aoki, S.-I. Kumamoto, and M. Yamada, Phase structure of NJL model with weak renormalization group, *Nucl. Phys. B* **931**, 105 (2018), arXiv:1705.03273 [hep-th].

[40] A. Kurganov and E. Tadmor, New High-Resolution Central Schemes for Nonlinear Conservation Laws and Convection-Diffusion Equations, *Journal of Computational Physics* **160**, 241 (2000).

[41] P. Virtanen, R. Gommers, T. E. Oliphant, M. Haberland, T. Reddy, D. Cournapeau, E. Burovski, P. Peterson, W. Weckesser, J. Bright, S. J. van der Walt, M. Brett, J. Wilson, K. J. Millman, N. Mayorov, A. R. J. Nelson, E. Jones, R. Kern, E. Larson, C. J. Carey, I. Polat, Y. Feng, E. W. Moore, J. VanderPlas, D. Laxalde, J. Perktold, R. Cimrman, I. Henriksen, E. A. Quintero, C. R. Harris, A. M. Archibald, A. H. Ribeiro, F. Pedregosa, P. van Mulbregt, and SciPy 1.0 Contributors, SciPy 1.0: Fundamental Algorithms for Scientific Computing in Python, *Nature Methods* **17**, 261 (2020).

[42] F. Ihssen, F. R. Sattler, and N. Wink, Numerical RG-time integration of the effective potential: Analysis and benchmark, *Phys. Rev. D* **107**, 114009 (2023), arXiv:2302.04736 [hep-th].

[43] J. Braun *et al.*, Soft modes in hot QCD matter, arXiv:2310.19853 [hep-ph] (2023).

[44] J. Braun, B. Klein, and P. Piasiecki, On the scaling behavior of the chiral phase transition in QCD in finite and infinite volume, *Eur. Phys. J. C* **71**, 1576 (2011), arXiv:1008.2155 [hep-ph].

[45] *fQCD Collaboration*: J. Braun, Y.-r. Chen, W.-j. Fu, F. Gao, F. Ihssen, A. Geissel, C. Huang, Y. Lu, J. M. Pawłowski, F. Rennecke, F. Sattler, B. Schallmo, J. Stoll, Y.-y. Tan, S. Töpfel, J. Turnwald, R. Wen, J. Wessely, N. Wink, S. Yin, N. Zorbach (December 2023).

[46] G. Van Rossum and F. L. Drake, *Python 3 Reference Manual* (CreateSpace, Scotts Valley, CA, 2009).

[47] J. D. Hunter, Matplotlib: A 2d graphics environment, *Computing in Science & Engineering* **9**, 90 (2007).

[48] C. R. Harris, K. J. Millman, S. J. van der Walt, R. Gommers, P. Virtanen, D. Cournapeau, E. Wieser, J. Taylor, S. Berg, N. J. Smith, R. Kern, M. Picus, S. Hoyer, M. H. van Kerkwijk, M. Brett, A. Haldane, J. F. del Río, M. Wiebe, P. Peterson, P. Gérard-Marchant, K. Sheppard, T. Reddy, W. Weckesser, H. Abbasi, C. Gohlke, and T. E. Oliphant, Array programming with NumPy,

Nature **585**, 357 (2020).

[49] W. R. Inc., **Mathematica, Version 12.1**, champaign, IL, 2023.